Cell Metabolism
Article

Comparative Metabolomics Reveals Endogenous Ligands of DAF-12, a Nuclear Hormone Receptor, Regulating *C. elegans* Development and Lifespan

Parag Mahanti,[1,6] Neelanjan Bose,[1,6] Axel Bethke,[1] Joshua C. Judkins,[1] Joshua Wollam,[2] Kathleen J. Dumas,[3] Anna M. Zimmerman,[1] Sydney L. Campbell,[1] Patrick J. Hu,[3,4] Adam Antebi,[2,5] and Frank C. Schroeder[1,*]
[1]Boyce Thompson Institute and Department of Chemistry and Chemical Biology, Cornell University, Ithaca, NY 14853, USA
[2]Max Planck Institute for Biology of Ageing, Joseph Stelzmann Strasse 9b, 50931 Cologne, Germany
[3]Life Sciences Institute, University of Michigan, Ann Arbor, MI 48109, USA
[4]Departments of Internal Medicine and Cell and Developmental Biology, University of Michigan Medical School, Ann Arbor, MI 48109, USA
[5]Huffington Center on Aging, Department of Molecular and Cellular Biology, Baylor College of Medicine, One Baylor Plaza, Houston, TX 77030, USA
[6]These authors contributed equally to this work
*Correspondence: schroeder@cornell.edu
http://dx.doi.org/10.1016/j.cmet.2013.11.024

SUMMARY

Small-molecule ligands of nuclear hormone receptors (NHRs) govern the transcriptional regulation of metazoan development, cell differentiation, and metabolism. However, the physiological ligands of many NHRs remain poorly characterized, primarily due to lack of robust analytical techniques. Using comparative metabolomics, we identified endogenous steroids that act as ligands of the *C. elegans* NHR, DAF-12, a vitamin D and liver X receptor homolog regulating larval development, fat metabolism, and lifespan. The identified molecules feature unexpected chemical modifications and include only one of two DAF-12 ligands reported earlier, necessitating a revision of previously proposed ligand biosynthetic pathways. We further show that ligand profiles are regulated by a complex enzymatic network, including the Rieske oxygenase DAF-36, the short-chain dehydrogenase DHS-16, and the hydroxysteroid dehydrogenase HSD-1. Our results demonstrate the advantages of comparative metabolomics over traditional candidate-based approaches and provide a blueprint for the identification of ligands for other *C. elegans* and mammalian NHRs.

INTRODUCTION

Small-molecule ligands of nuclear hormone receptors (NHRs), a conserved family of ligand-activated transcription factors, control diverse aspects of metabolism, cell differentiation, development, and aging. Precise knowledge of ligand structures and biosynthetic pathways is essential for understanding NHR function (Mangelsdorf et al., 1995; Wollam and Antebi, 2011) because even small differences in ligand structures may result in dramatic changes of transcriptional activity and specificity (Brown and Slatopolsky, 2008; Singarapu et al., 2011). However, the endogenous ligands of many NHRs remain poorly characterized, in part because ligands constitute very minor components of highly complex animal metabolomes (Schupp and Lazar, 2010). The free-living nematode *C. elegans* has 284 NHRs, allows facile genetic manipulation, and can be grown in large quantities, providing an opportunity to investigate structures, biosynthesis, and functions of NHR ligands in a relatively simple model system (Taubert et al., 2011). Although many of the 284 *C. elegans* NHRs appear to be derived from extensive duplication and diversification of an ancestral gene related to mammalian hepatocyte nuclear factor 4 (HNF4) receptors and may not be ligand regulated, several *C. elegans* NHRs represent orthologs of hormone-regulated NHRs in other metazoans (Antebi, 2006; Palanker et al., 2009; Taubert et al., 2011). The most prominent *C. elegans* NHR, DAF-12, a homolog of vertebrate vitamin D and liver X receptors (VDR and LXR, respectively), functions as a ligand-dependent switch that regulates both adult lifespan and larval development (Antebi et al., 2000; Fielenbach and Antebi, 2008; Kenyon, 2010; Riddle et al., 1981; Riddle and Albert, 1997; Shen et al., 2012). The biosynthesis of the steroidal ligands of DAF-12 is controlled by a complex endocrine signaling network, of which many components appear to be conserved between *C. elegans* and mammals (Fielenbach and Antebi, 2008). Perception of environmental stimuli by chemosensory neurons modulates conserved insulin/IGF and transforming growth factor β (TGF-β) signaling pathways, which converge on genes implicated in DAF-12 ligand biosynthesis (Figure 1A). Under unfavorable conditions, such as overcrowding or scarcity of food, ligand biosynthesis is suppressed, and unliganded DAF-12 interacts with its corepressor DIN-1 (Ludewig et al., 2004). The resulting repression of DAF-12 target genes causes developmental arrest and entry into a highly stress-resistant larval stage called the dauer diapause (Gems et al., 1998; Hu, 2007; Larsen et al., 1995; Schaedel et al., 2012). In contrast, favorable conditions trigger upregulation of DAF-12 ligand biosynthesis. DAF-12 ligand binding then results in dissociation of the corepressor DIN-1 to allow expression of DAF-12 target genes, promoting rapid development from larvae to reproductive adults

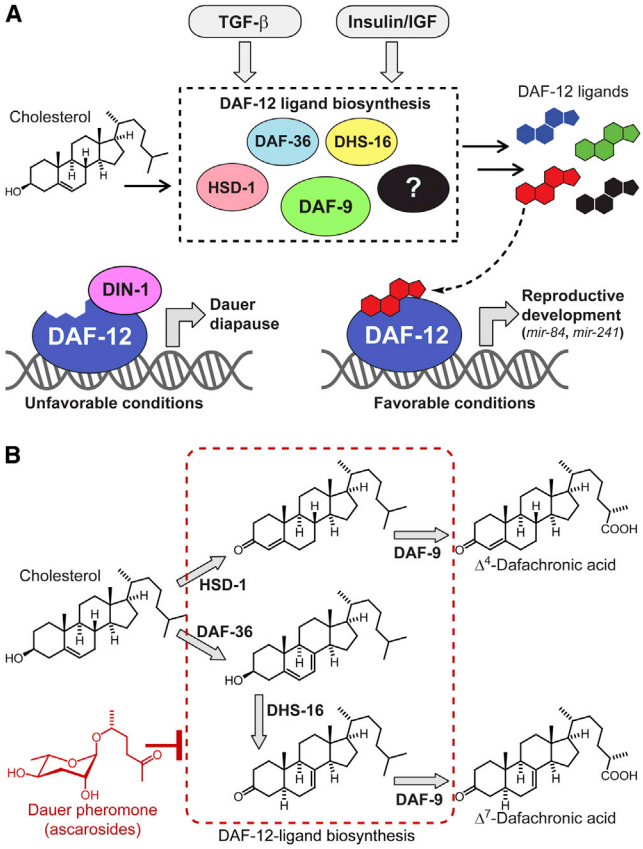

Figure 1. Steroidal Ligands Control *C. elegans* Development and Lifespan via the Nuclear Hormone Receptor DAF-12

(A) Under favorable conditions, insulin/IGF and TGF-β signaling drive biosynthesis of steroidal DAF-12 ligands. Liganded DAF-12 promotes development, in part via transcription of the *let-7* family microRNAs *mir-84* and *mir-241*. Under unfavorable conditions, ligand biosynthesis is inhibited, resulting in interaction of unliganded DAF-12 with its corepressor DIN-1.

(B) Previously described DAF-12 ligands and proposed biosynthetic pathways. DAF-12 ligand biosynthesis is downregulated in response to dauer pheromone, a blend of ascarosides (e.g., the shown ascr#2; red).

(Fielenbach and Antebi, 2008; Ludewig et al., 2004). Additionally, ligand-dependent activation of the DAF-12 target genes *mir-84* and *mir-241*, two microRNAs of the conserved *let-7* family (Bethke et al., 2009; Hammell et al., 2009), is required for lifespan regulation in response to signals from reproductive tissues (Shen et al., 2012; Yamawaki et al., 2010). These findings indicate that metazoan lifespan is coupled to the gonad via NHR signaling.

Based on extensive biochemical studies, two bile acid-like steroids named Δ^4- and Δ^7-dafachronic acid (DA) were proposed as endogenous ligands of DAF-12 (Figure 1B) (Motola et al., 2006). Identification of the DAs as DAF-12 ligand candidates was based on precursor studies in which a variety of 3-keto sterols were identified as substrates for the cytochrome P450, DAF-9, which had been shown to act upstream of DAF-12 in DAF-12 ligand biosynthesis (Gerisch et al., 2001; Jia et al., 2002; Motola et al., 2006). DAF-9 was further shown to act on the side chain in these steroids, introducing a terminal carboxyl group (Motola et al., 2006). In a separate study, a DAF-12-activating isomer of 3β-hydroxy-5-cholestenoic acid was detected in *C. elegans* metabolite extracts (Held et al., 2006). However, given the very low concentrations of the putative DAF-12 ligands in *C. elegans*, isolation and full spectroscopic characterization of these compounds was not pursued.

Although none of the structures of the proposed DAF-12 ligands have been confirmed based on conclusive spectroscopic analysis of *C. elegans*-derived samples, a biosynthesis model has been developed (Figure 1B), and the biochemical roles of genes proposed to function upstream of DAF-9 in DAF-12 ligand biosynthesis have been studied extensively (Dumas et al., 2010; Gerisch et al., 2007; Patel et al., 2008; Rottiers et al., 2006; Williams et al., 2010; Wollam et al., 2011; Yoshiyama-Yanagawa et al., 2011). More recent work has shown that the proposed DAF-12 ligands do not explain all DAF-12-associated functions and suggested the possibility that other DAs may exist (Patel et al., 2008; Williams et al., 2010; Wollam et al., 2012). In this study, we identify the endogenous ligands of DAF-12 using an unbiased comparative metabolomics approach (Forseth and Schroeder, 2011), which revealed ligand structures and differential regulation of DAF-12 ligand biosynthesis.

RESULTS

Customizing a Comparative Metabolomics Approach

We aimed to identify endogenous DAF-12 ligands from direct spectroscopic evidence, in contrast to earlier work that relied on classical genetics and biochemical experiments. For this purpose, we combined activity-guided fractionation and NMR-based comparative metabolomics via DANS (differential analyses by 2D NMR spectroscopy) (Figure 2A). 2D NMR spectroscopy can provide a largely unbiased overview of metabolome composition, and comparing 2D NMR spectra of different mutant backgrounds via DANS often permits detection and partial identification of minor metabolites such as signaling molecules (Forseth and Schroeder, 2011; Pungaliya et al., 2009). DANS relies on correlating genetic changes with metabolomic changes for compound identification, thereby reducing the need for extensive fractionation, which can result in activity loss or the introduction of artifacts. We envisioned that this strategy could be applied to identify DAF-12 ligands if one compared a mutant metabolome lacking DAF-12 ligands with the metabolome of worms that produce DAF-12 ligands abundantly.

For DANS-based ligand identification, we chose *daf-9;daf-12* double mutants as the ligand-deficient strain and *daf-22* mutants as a putatively ligand-rich reference strain. *daf-9;daf-12* double mutants do not produce DAF-12 ligands, but nonetheless bypass the dauer stage, because lack of DAF-12 prevents the execution of genetic programs required for dauer formation (Gerisch and Antebi, 2004). Therefore, these animals can be grown in quantities large enough for NMR spectroscopic analyses. *daf-22* mutant worms develop normally to adulthood but are defective in the biosynthesis of the dauer-inducing ascarosides (Butcher et al., 2009; von Reuss et al., 2012), which we hypothesized may adversely affect DAF-12 ligand production in wild-type (WT) liquid cultures (Figure 1B). Downregulation of DAF-12 ligand biosynthesis by ascarosides is also suggested by the finding that exposure to high concentrations of dauer pheromone abolished expression of DAF-9, one of the key

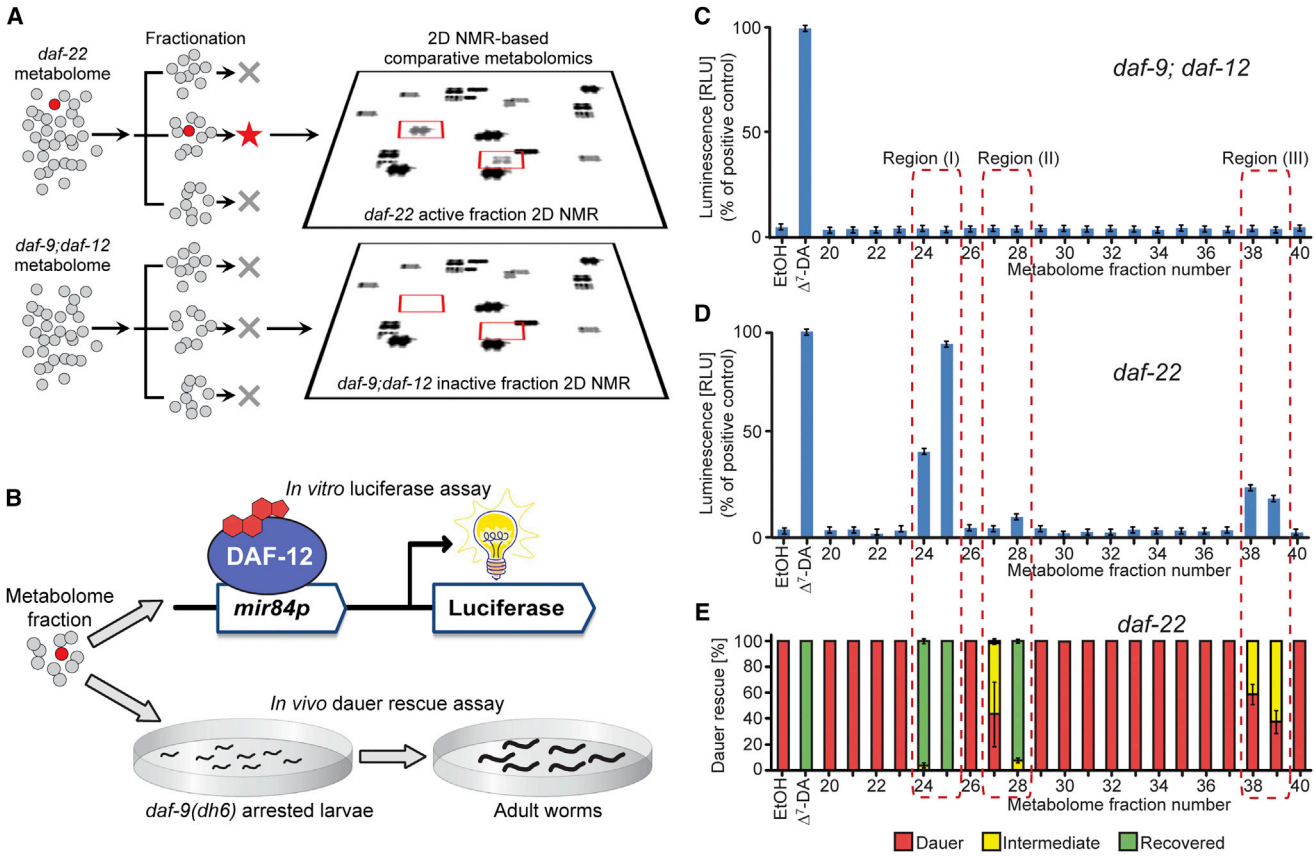

Figure 2. Detection of DAF-12 Ligands in *C. elegans* Mutant Metabolomes

(A) Fractionation of active, ligand-rich *daf-22* and inactive *daf-9;daf-12* metabolomes is followed by 2D NMR-based comparative metabolomics of active fractions.

(B) Assessment of DAF-12 ligand content using (1) an in vitro luciferase assay in HEK293T cells transfected with full-length DAF-12 and a *mir84p*-luciferase reporter vector and (2) in vivo *daf-9(dh6)* dauer rescue assays.

(C) *daf-9;daf-12* metabolome fractions are inactive in the luciferase assay. We used 100 nM Δ^7-DA as a positive control (error bars, ± SD).

(D) Luciferase assays of *daf-22* metabolome fractions reveal three active regions (error bars, ± SD).

(E) *daf-9(dh6)* dauer rescue assays of *daf-22* metabolome fractions show activity in the same three regions (error bars, ± SD). For worm images of scored phenotypes, see Figure S1C. See also Figure S1.

enzymes in the proposed biosynthetic pathway of DAF-12 ligands (Schaedel et al., 2012). Furthermore, given that the mammalian ortholog of DAF-22, SCPx, is involved in oxidative breakdown of steroid side chains in bile acid biosynthesis, it seemed possible that DAF-22 contributes to degradation of steroidal DAF-12 ligands in *C. elegans*.

To prepare for DANS analysis, metabolome extracts of *daf-9; daf-12*, WT, and *daf-22* mixed-stage liquid cultures were fractionated using an automated, highly reproducible chromatography system (Figure 2A and Supplemental Experimental Procedures). The resulting parallel sets of metabolome fractions were assessed for DAF-12 ligand content using in vivo and in vitro bioassays (Figure 2B). The in vivo assay used *daf-9(dh6)* worms, which are defective in DAF-12 ligand production. In the absence of exogenously added DAF-12 ligand or a suitable precursor, developing *daf-9(dh6)* worms arrest as dauer larvae because unliganded DAF-12 constitutively interacts with its corepressor DIN-1 (Gerisch et al., 2007; Ludewig et al., 2004). The assay scored the ability of added fractions to rescue the arrested dauer larvae and promote development to adulthood, providing a measure for the presence of a DAF-12 ligand that would dissociate the DAF-12/DIN-1 complex. The in vitro assay measured transcriptional activation by DAF-12 of a luciferase reporter in human embryonic kidney 293T (HEK293T) cells that were cotransfected with full-length DAF-12 and the reporter construct (Bethke et al., 2009). This assay provided a measure for ligand-dependent interaction of DAF-12 with mammalian coactivator(s) in the cells. Both of these assays consistently showed activity for three groups of *daf-22* and WT fractions (regions I–III in Figures 2C–2E; for WT assay data, see Figure S1 available online), indicating the presence of DAF-12 ligands or precursors, whereas all *daf-9;daf-12* fractions were inactive in both assays, in accordance with previous work (Gerisch and Antebi, 2004; Gerisch et al., 2007; Motola et al., 2006). As anticipated, *daf-22* fractions were significantly more active in the *daf-9(dh6)* dauer rescue assay compared to the corresponding WT fractions, suggesting higher production of DAF-12 ligands in *daf-22* mutants (Figure S1).

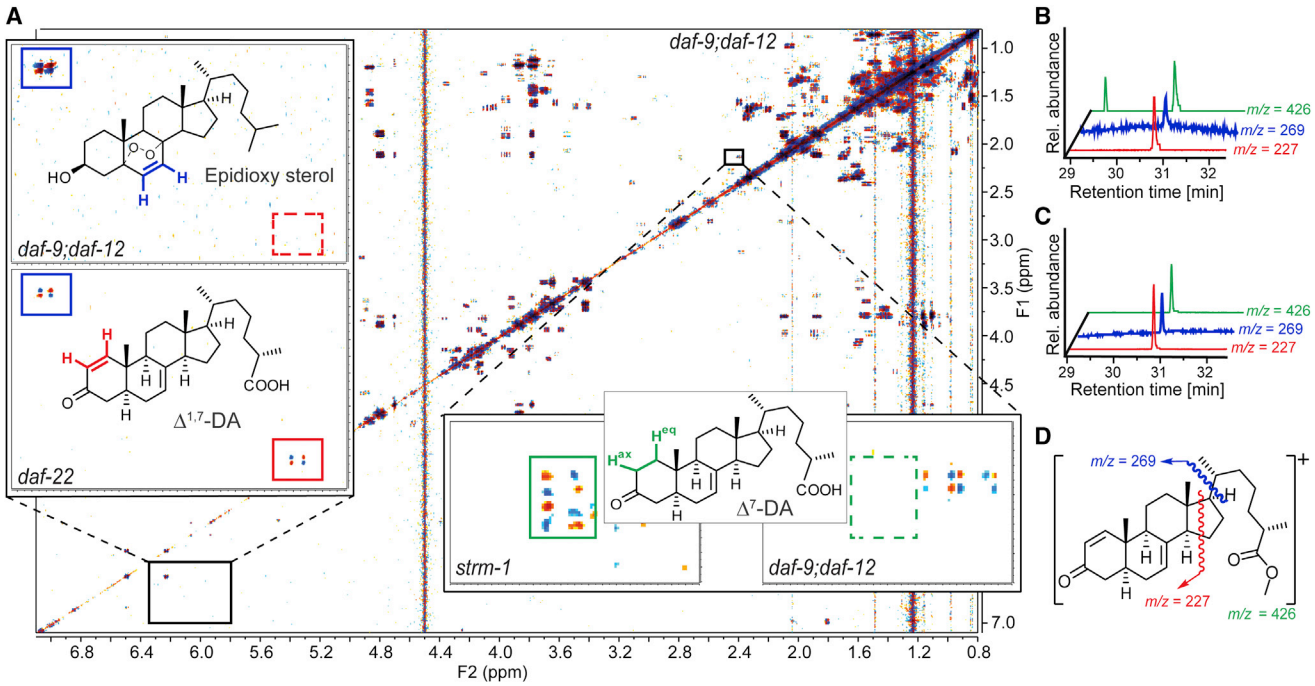

Figure 3. Detection and Identification of Endogenous DAF-12 Ligand Candidates via 2D NMR-Based Comparative Metabolomics and SIM GC-MS

(A) DQF-COSY spectrum of inactive *daf-9;daf-12* metabolome fraction corresponding to active region I (Figures 2C–2E). Enlarged section (upper left) compares *daf-9;daf-12* with the corresponding section of the *daf-22* spectrum, showing one of the differential cross-peaks (red) that led to identification of $\Delta^{1,7}$-DA, next to nondifferential signals representing a metabolite present in both *daf-9;daf-12* and *daf-22*, an epidioxy sterol (blue). Enlarged section (lower right) shows example cross-peaks from the comparison of the spectra of *strm-1* (vide infra) and *daf-9;daf-12* metabolomes, showing signals (green) characteristic for Δ^{7}-DA in the *strm-1* spectrum, but not the *daf-9;daf-12* spectrum.

(B) SIM GC-MS of active *daf-22* metabolome fraction indicating the presence of $\Delta^{1,7}$-DA. The additional peak at ~29.4 min in the ion trace *m/z* = 426 belongs to an unrelated compound.

(C) SIM GC-MS of synthetic $\Delta^{1,7}$-DA confirms retention times and fragmentation patterns.

(D) Major electron ionization-mass spectrometry (EI-MS) fragments of $\Delta^{1,7}$-DA used in Figures 3B and 3C. See also Figure S2. For NMR spectroscopic data, see Tables S1 and S2.

DANS Reveals Steroids with Unexpected Structural Features

2D NMR spectra of the most active group of *daf-22* fractions, active region I, revealed long-chained ascarosides (Pungaliya et al., 2009) in addition to a complex mixture of fatty acids, glycerides, other lipids, and epidioxy sterol derivatives (Figures 3A and S2A), all of which were also present in similar concentrations in corresponding *daf-9;daf-12* fractions. Closer inspection of region I 2D NMR spectra revealed several sets of signals that were consistently absent in *daf-9;daf-12* and thus appeared to be *daf-9* dependent (Figure 3A). Further analysis of these differential signals suggested that they represent steroidal structures. Because of their very low concentrations, identification of the putative *daf-9*-dependent steroids required additional fractionation via high-performance liquid chromatography (HPLC), which resulted in two active samples, each containing 1%–2% of *daf-9*-dependent components (Figures S2B and S2C). NMR spectroscopic analysis of the most active fractions showed a distinct set of *daf-9*-dependent signals at 5.9 and 7.0 ppm with a coupling constant of 10 Hz, which indicated the presence of an unusual Δ^{1}-unsaturated 3-ketosteroid (Figure 3A). Comparison with published data suggested the presence of 3-oxo-1,7-cholestadienoic acid ($\Delta^{1,7}$-DA), which had not previously been described from worms, in addition to smaller amounts of the known Δ^{7}-DA (Figures 3A and 4A) (Motola et al., 2006). These assignments were confirmed by comparison of spectroscopic data and gas chromatography-mass spectrometry (GC-MS) retention times with those of synthetic samples of $\Delta^{1,7}$-DA and Δ^{7}-DA (Figures 3B, 3C, and S2D–S2I). To determine the relative configuration of the chiral centers at position 25 in the side chains of Δ^{7}-DA and $\Delta^{1,7}$-DA, we compared the NMR spectra of synthetic samples of (25*S*)- and (25*R*)-diastereomers with those of the natural samples. These analyses established the configuration of natural Δ^{7}-DA and $\Delta^{1,7}$-DA as (25*S*) (Figure 4). Δ^{1}-unsaturated steroids are rare in nature, and we are aware of only one other example in animals (Wang et al., 2009a).

Comparative analysis of active region II led to the identification of another *daf-9*-dependent cholestenoic acid derivative, featuring unusual 3α-hydroxylation: (25*S*)-3α-hydroxy-7-cholestenoic acid (3α-OH-Δ^{7}-DA) (Figures 4A and S2J–S2O). The GC-MS fragmentation pattern of 3α-OH-Δ^{7}-DA suggests that it is identical to the unidentified isomer of (25*S*)-3β-cholestenoic acid previously reported as a DAF-12 ligand by Held et al. (2006) (Figure S2K). As all 3-hydroxylated steroids previously

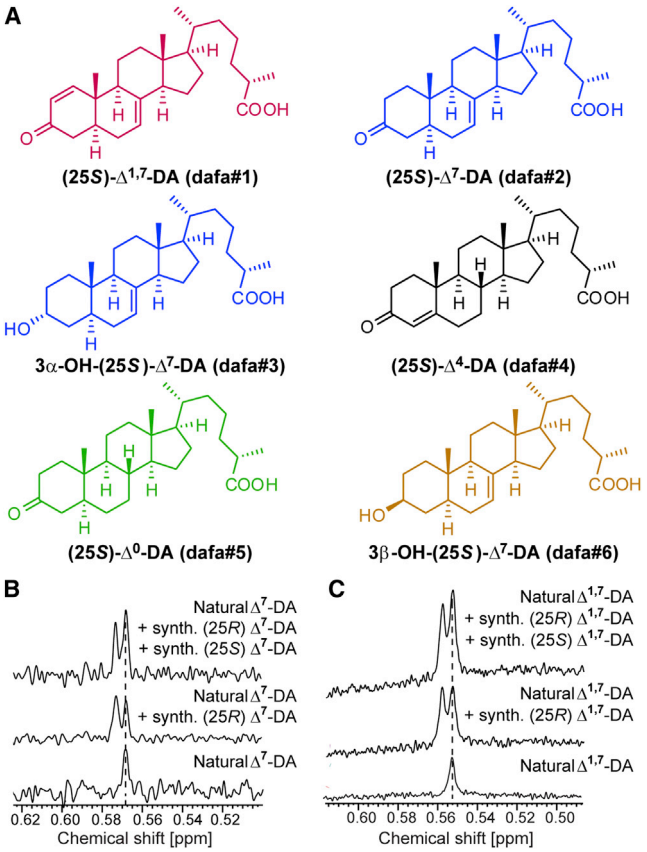

Figure 4. Structures and ^{1}H-NMR-Based Assignment of Absolute Configuration of DAF-12 Ligands

(A) Structures of $\Delta^{1,7}$-DA (dafa#1), Δ^7-DA (dafa#2), 3α-OH-Δ^7-DA (dafa#3), Δ^4-DA (dafa#4), Δ^0-DA (dafa#5), and 3β-OH-Δ^7-DA (dafa#6). See Experimental Procedures for compound nomenclature.

(B) NMR spectroscopic determination of the relative configuration at C-25 in natural Δ^7-DA. C-18 singlet region of ^{1}H NMR spectra (600 MHz, pyridine-d_5) of natural Δ^7-DA and mixtures with synthetic (25*R*)-Δ^7-DA and (25*S*)-Δ^7-DA.

(C) NMR spectroscopic determination of the relative configuration at C-25 in natural $\Delta^{1,7}$-DA. C-18 singlet region of ^{1}H NMR spectra (600 MHz, pyridine-d_5) of natural $\Delta^{1,7}$-DA and mixtures with synthetic (25*R*)-$\Delta^{1,7}$-DA and synthetic (25*S*)-$\Delta^{1,7}$-DA.

described from *C. elegans* feature 3β configuration, the identification of 3α-OH-Δ^7-DA was surprising. We then inspected both active and inactive *C. elegans* metabolome fractions for the presence of the corresponding 3β stereoisomer, 3β-OH-Δ^7-DA (Figure 4A); however, 3β-OH-Δ^7-DA could not be detected in either WT or *daf-22* metabolomes, indicating that production of 3α-OH-Δ^7-DA is highly selective. Active region III, representing a series of metabolome fractions with weak *daf-9(dh6)* dauer rescue activity, revealed trace quantities of glucosides of DAs that were not characterized further.

$\Delta^{1,7}$-DA and Δ^7-DA Are Potent DAF-12 Ligands

Next, we investigated the biological properties of synthetic samples of the identified *daf-9*-dependent steroids (Figures 5A–5D). Synthetic $\Delta^{1,7}$-DA activated DAF-12 in mammalian cells (half-maximal effective concentration [EC_{50}] = 146 nM), and its potency in the *daf-9(dh6)* dauer rescue assay was similar (EC_{50} = 2 nM) or slightly higher than that of Δ^7-DA (Figure 5B and Table S3). Similarly, 3α-OH-Δ^7-DA was active in both the in vivo and in vitro assays, whereas its 3β-stereoisomer did not activate DAF-12 in mammalian cells at any tested concentration and rescued the *daf-9(dh6)* dauer phenotype only at very high concentrations (Figure 5B). We also assayed the two most abundant *daf-9*-dependent compounds for their effect on lifespan in germline-deficient *glp-1* mutant worms. Germline-deficient *glp-1* mutant worms live up to 60% longer than WT, and this lifespan extension has been shown to depend on functional DAF-12 and DAF-12 ligand biosynthetic enzymes (Gerisch et al., 2001; Hsin and Kenyon, 1999; Yamawaki et al., 2010). Correspondingly, ligand-deficient *glp-1;daf-36* double-mutant worms lack the *glp-1* lifespan phenotype (Gerisch et al., 2007; Rottiers et al., 2006). We found that both Δ^7-DA and $\Delta^{1,7}$-DA fully restore *glp-1*-dependent lifespan extension to *glp-1;daf-36* worms (Figures 5C and S3A).

For quantification of the identified *daf-9*-dependent steroids, we employed selective ion monitoring (SIM) GC-MS detection of characteristic MS fragments of volatile methylated or silylated derivatives (Supplemental Experimental Procedures). SIM GC-MS showed that $\Delta^{1,7}$-DA is slightly more abundant than Δ^7-DA in *daf-22* worms, whereas in WT animals, $\Delta^{1,7}$-DA is more than twice as abundant as Δ^7-DA, with concentrations (averaged over the worm bodies) of 93 nM and 197 nM for Δ^7-DA and $\Delta^{1,7}$-DA, respectively (Figure 5E). 3α-OH-Δ^7-DA occurs at concentrations about 3- to 5-fold lower than those of Δ^7-DA in both WT and *daf-22* mutants. Based on the specific activities determined for synthetic samples of Δ^7-DA, $\Delta^{1,7}$-DA, and 3α-OH-Δ^7-DA, it appears that these three compounds account for all of the activity in regions I and II in both the WT and *daf-22* metabolomes. Using SIM GC-MS, we also checked the *daf-22* and WT metabolomes for the presence of the previously reported Δ^4-DA. We were unable to detect Δ^4-DA in any of our *C. elegans* metabolome fractions, whereas fractions spiked with trace quantities of synthetic Δ^4-DA confirmed the sensitivity of our detection methods (Figure S2P). We then considered that our growth conditions may have affected production of the putative precursor of Δ^4-DA, 4-cholesten-3-one (Motola et al., 2006; Patel et al., 2008). However, analysis of WT metabolome samples by GC-MS and NMR spectroscopy revealed that 4-cholesten-3-one is as abundant as lathosterone (Figures S2Q–S2V), a putative precursor of Δ^7-DA (Motola et al., 2006; Wollam et al., 2012), suggesting that absence of Δ^4-DA is not the result of a lack of suitable precursors. Therefore, it appears that Δ^4-DA may not play a significant role as a DAF-12 ligand, although its transient or very-low-level production cannot be excluded.

To test whether the identified *daf-9*-dependent compounds constitute bona fide ligands of DAF-12, we measured ligand-dependent binding of DAF-12 with the SRC1-4 peptide containing the nuclear receptor box (NR box) motif of mammalian coactivator SRC-1 (Heery et al., 1997). We found that Δ^7-DA, $\Delta^{1,7}$-DA, and 3α-OH-Δ^7-DA affect concentration-dependent recruitment of SRC1-4, with EC_{50} values of 8 nM and 15 nM for Δ^7-DA and $\Delta^{1,7}$-DA, respectively, whereas affinity of 3α-OH-Δ^7-DA was lower (EC_{50} = 200 nM, Figure 5D and Table S3). These relative potencies of Δ^7-DA, $\Delta^{1,7}$-DA, and 3α-OH-Δ^7-DA are similar to relative activities observed in the luciferase assay (Figure 5A).

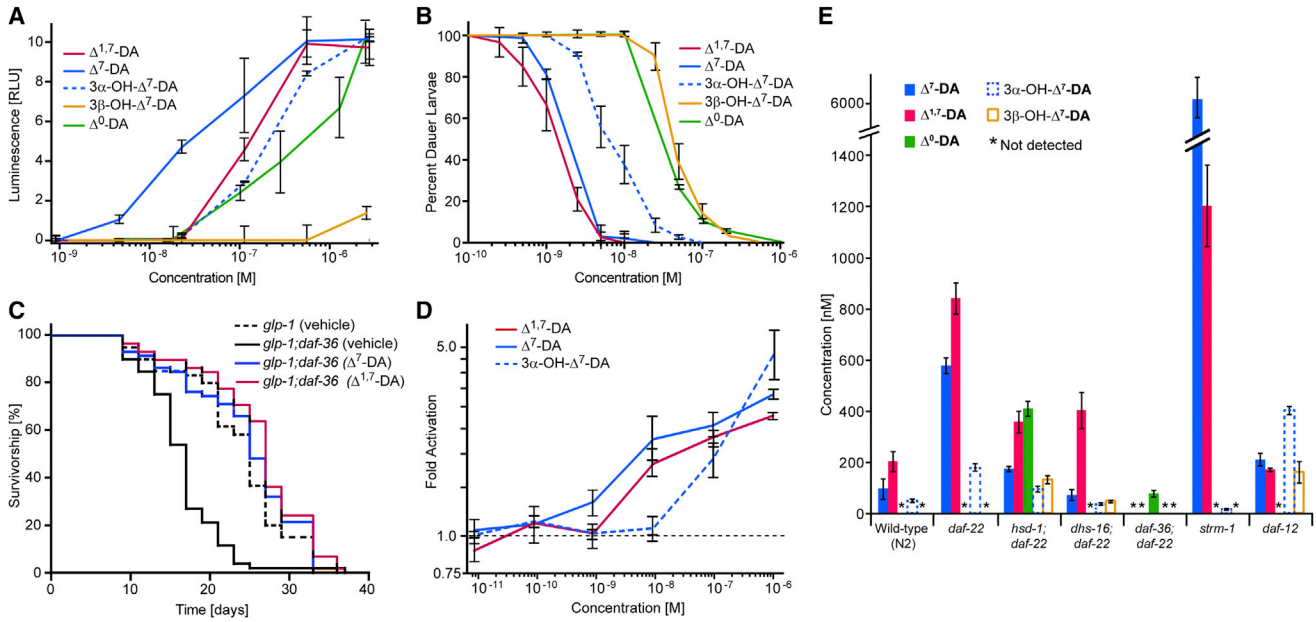

Figure 5. Biological Activities of DAF-12 Ligands and Quantification of DAF-12 Ligands in *C. elegans* WT, Steroid Metabolism Mutant, and *daf-12(0)* Mutant Worms

(A) DAF-12 transcriptional activation in HEK293T cells by the identified endogenous DAF-12 ligand candidates. Luciferase assays were measured in triplicates (error bars, ± SD).

(B) *daf-9(dh6)* dauer rescue with the identified endogenous DAF-12 ligand candidates at 27°C. For each data point, there were two replicates with 100 animals per replicate (error bars, ± SD).

(C) Both Δ^7-DA (100 nM) and $\Delta^{1,7}$-DA (100 nM) restore lifespan extension to *glp-1* animals in *daf-36* null mutant background.

(D) AlphaScreen assay for ligand-dependent recruitment of SRC1-4 peptide by DAF-12, showing fold activation of DAF-12 with different ligand candidates over ethanol control (error bars, SEM).

(E) In vivo concentrations of the identified endogenous dafachronic acids in WT (N2), *daf-22*, *daf-12*, and steroid metabolism mutants (error bars, ± SD) grown in mixed-stage liquid cultures, as determined from SIM GC-MS analysis of metabolome fractions (for distribution of life stages at the time of harvesting, see Figure S3R). Detection limits for SIM GC-MS-based quantification of dafachronic acids in these experiments were around 2.5 nM. See also Figure S3.

Taken together, these results indicate that $\Delta^{1,7}$-DA and Δ^7-DA are high-affinity ligands of DAF-12 that promote reproductive development and adult longevity, whereas 3α-OH-Δ^7-DA is of lower potency in promoting these phenotypes, and Δ^4-DA may not be present at physiologically relevant concentrations. Therefore, previous hypotheses about DAF-12 ligand structures and their biosynthetic pathways must be revised.

Comparative Metabolomics Suggests Tissue-Specific Ligand Biosynthesis

Using our comparative metabolomics strategy, we reinvestigated the roles of four additional enzymes that have been proposed to participate in DAF-12 ligand biosynthesis. In a recent model (Figure 1B), DAF-12 ligand biosynthesis begins with oxidation of cholesterol by the Rieske-like oxygenase, DAF-36, yielding 7-dehydrocholesterol (Wollam et al., 2011; Yoshiyama-Yanagawa et al., 2011). 7-dehydrocholesterol is converted by an unknown enzyme to lathosterol, which is oxidized to the corresponding ketone, lathosterone, by the short-chain dehydrogenase DHS-16 (Wollam et al., 2012). Lathosterone is then converted to Δ^7-DA by DAF-9 (Gerisch et al., 2007; Motola et al., 2006). In addition, a parallel pathway for the biosynthesis of Δ^4-DA, involving the putative hydroxysteroid dehydrogenase HSD-1, has been proposed (Dumas et al., 2010; Patel et al., 2008). However, recent evidence suggests that HSD-1 has no role in the production of the putative precursor of Δ^4-DA, 4-cholesten-3-one (Wollam et al., 2012), leaving its role in DAF-12 ligand biosynthesis undetermined. Therefore, we began our biosynthetic analysis with profiling *hsd-1* mutants and *hsd-1;daf-22* double mutants. Whereas *hsd-1* fractions contained only very small amounts of dauer rescuing activity, the activity profile of *hsd-1;daf-22* fractions was similar to that of *daf-22* fractions, consistent with the hypothesis that dauer pheromone biosynthesis via DAF-22 downregulates DAF-12 ligand production (Figure S3D). However, comparative 2D NMR analysis of *hsd-1;daf-22* region I revealed production of large quantities of an additional steroid in *hsd-1;daf-22* worms that is not produced in either *daf-22* or *daf-9;daf-12* mutants. Comparison with a synthetic sample led to the identification of this *hsd-1*-specific steroid as (25*S*)-3-keto-cholestanoic acid (Δ^0-DA; Figures 4A and S3G–S3K). This fully saturated DA derivative is active in both the DAF-12 luciferase assay and the *daf-9(dh6)* dauer rescue assay, although its activity is lower than that of $\Delta^{1,7}$-DA and Δ^7-DA (Figures 5A and 5B). Δ^0-DA was absent in WT and *daf-22* metabolomes, as determined by NMR and SIM GC-MS. Analysis of *hsd-1;daf-22* activity region II revealed a second *hsd-1*-specific steroid, 3β-OH-Δ^7-DA (Figure S3L). In *hsd-1;daf-22* mutants, 3β-OH-Δ^7-DA is as abundant as the 3α isomer, whereas 3β-OH-Δ^7-DA is absent in both WT and *daf-22* mutants. GC-MS analysis of *hsd-1;daf-22* activity region

I further revealed that the amounts of both $\Delta^{1,7}$-DA and Δ^{7}-DA are slightly reduced compared to *daf-22* worms, whereby production of Δ^{7}-DA may be more strongly affected than that of $\Delta^{1,7}$-DA (Figure 5E).

The identification of 3β-OH-Δ^{7}-DA and Δ^{0}-DA in *hsd-1;daf-22* mutant worms suggests that HSD-1 may directly or indirectly participate in the biosynthesis of Δ^{7}-DA and possibly $\Delta^{1,7}$-DA. HSD-1 has homology to mammalian 3β-hydroxysteroid dehydrogenases (Patel et al., 2008), which suggested its participation in introducing the 3-keto functionality in Δ^{4}-DA. The absence of Δ^{4}-DA and our identification of Δ^{0}-DA as a shunt metabolite in *hsd-1;daf-22* mutants may indicate that the *hsd-1* pathway includes introduction of the 7,8-double bond in a saturated precursor (for example, cholestanol, 3β-OH-Δ^{0}-DA, or Δ^{0}-DA) by an unknown enzyme or that HSD-1 itself has 7-dehydrogenase activity. Notably, HSD-1 is expressed mainly in the neuron-like XXX cells, which lack expression of the oxygenase DAF-36 required for biosynthesis of most 7,8-unsaturated steroids in *C. elegans* (Wollam et al., 2011; Yoshiyama-Yanagawa et al., 2011). Taken together, our results suggest that HSD-1 contributes to Δ^{7}-DA biosynthesis in the XXX cells but that Δ^{7}-DA and $\Delta^{1,7}$-DA are produced via a separate pathway in other tissues.

Next, we investigated the DAF-12 ligand profile of mutants of the Rieske oxygenase, DAF-36 (Figure 1B) (Wollam et al., 2011; Yoshiyama-Yanagawa et al., 2011). Mutants of *daf-36*, which is expressed primarily in the worm intestine, exhibit phenotypes consistent with strongly reduced DAF-12 ligand biosynthesis, such as a higher tendency to enter dauer (Rottiers et al., 2006). As in the case of *hsd-1* mutants, *daf-36* mutant metabolome fractions were largely inactive in the dauer rescue and luciferase assays, whereas *daf-36;daf-22* double mutants produced significant dauer rescue activity in region I (Figure S3E). GC-MS analysis revealed the presence of saturated Δ^{0}-DA in this region (Figures S3M–S3O), which we previously found only in *hsd-1;daf-22* mutants. In contrast to *hsd-1;daf-22* mutants, Δ^{0}-DA appears to be responsible for all activity observed in *daf-36;daf-22* region I, and neither Δ^{7}-DA nor $\Delta^{1,7}$-DA was detectable in this mutant. Total DAF-12 ligand amounts were much lower in the *daf-36;daf-22* metabolome than in *hsd-1;daf-22* (Figure 5E). These results indicate that the intestinally expressed 7,8-dehydrogenase, DAF-36, is required for Δ^{7}-DA and $\Delta^{1,7}$-DA biosynthesis, whereas HSD-1 contributes to additional production of Δ^{7}-unsaturated DAs in the XXX cells. Thus, it appears that biosynthesis of Δ^{7}-DA and $\Delta^{1,7}$-DA relies on partially redundant and tissue-specific pathways.

Biosynthesis of Different Ligands Is Differentially Regulated

Whereas the *hsd-1* mutation did not significantly affect the relative abundance of $\Delta^{1,7}$-DA and Δ^{7}-DA, mutations of two other genes involved in DAF-12 ligand biosynthesis and regulation, the short-chain dehydrogenase (*dhs-16*) (Wollam et al., 2012) and the methyltransferase (*strm-1*) (Hannich et al., 2009), showed strongly altered ligand ratios. Similar to what we observed for *daf-36* and *hsd-1* single mutants, bioassays of metabolome fractions from *dhs-16* single mutants showed very low activity, whereas *dhs-16;daf-22* double-mutant fractions showed levels of activity similar to those of *daf-22* fractions (Figure S3F). Chemical analysis of the *dhs-16;daf-22* fractions revealed that production of Δ^{7}-DA was greatly reduced compared to *daf-22* single mutants, whereas $\Delta^{1,7}$-DA levels were only slightly reduced (Figures 1B and 5E). These results indicate that $\Delta^{1,7}$-DA and Δ^{7}-DA may be derived from partially divergent biosynthetic pathways or that deletion of *dhs-16* indirectly affects regulation of the $\Delta^{1,7}$-DA:Δ^{7}-DA ratio. Only trace quantities of 3α-OH-Δ^{7}-DA were detected in *dhs-16;daf-22* worms, suggesting that production of both 3α-OH-Δ^{7}-DA and Δ^{7}-DA are DHS-16 dependent (Figure 5E). Next, we characterized the DAF-12 ligand profile of *strm-1* mutants (Figure S3F), which had previously been shown to produce elevated levels of DAF-12 ligands (Hannich et al., 2009). The methyltransferase STRM-1 regulates DAF-12 ligand levels by converting cholesterol-derived intermediates of ligand biosynthesis into 4-methylated steroids, thereby rendering them unsuitable as ligand precursors (Hannich et al., 2009). NMR spectroscopy and SIM GC-MS analyses revealed levels of Δ^{7}-DA increased more than 100-fold in *strm-1* metabolomes, whereas $\Delta^{1,7}$-DA levels increased only about 7-fold compared to WT (Figure 5E).

We also investigated the DAF-12 ligand profile of *daf-12* null mutants, which previously had been shown to produce increased dauer rescuing activity (Held et al., 2006). We found that, compared to WT, *daf-12* mutants produced amounts of 3α-OH-Δ^{7}-DA roughly 6-fold higher, whereas amounts of $\Delta^{1,7}$-DA and Δ^{7}-DA were only slightly increased (Figure 5E). In addition, *daf-12* mutants produce large quantities of 3β-OH-Δ^{7}-DA, whereas this compound could not be detected in WT. These observations indicate that DAF-12 ligand biosynthesis is dysregulated in *daf-12* null mutants, possibly as a result of changes in the expression levels of additional ligand biosynthetic (or catabolic) enzymes.

Given that DAF-12 ligands regulate both larval development and germline-dependent adult longevity, it seemed possible that different life stages may produce different ligand profiles. SIM GC-MS analysis of metabolite extract from synchronized larvae at the L2 and L3 stages showed a Δ^{7}-DA:$\Delta^{1,7}$-DA ratio of about 1:1, whereas in worms at the L4 and young adult stages, the ratio is shifted toward $\Delta^{1,7}$-DA (Figures S3P and S3Q). More detailed analysis of the ligand profiles of different life stages and under different environmental conditions will have to await development of more sensitive detection techniques, especially for the somewhat chemically unstable $\Delta^{1,7}$-DA. Taken together, our results indicate that the biosynthesis of different DAF-12 ligands is differentially regulated, in part via feedback through DAF-12.

DISCUSSION

Identification of the endogenous ligands of NHRs is central to understanding their role as transcriptional regulators in metazoans. Screening of synthetic ligands of the vitamin D receptor and other mammalian NHRs has demonstrated that even small changes in ligand structures can strongly affect gene transcription (Brown and Slatopolsky, 2008; Singarapu et al., 2011; Wollam and Antebi, 2011). However, there are few approaches to comprehensively identify the endogenous NHR ligands from complex animal metabolomes, whose chemical annotations remain largely incomplete. In this study, we demonstrate the use of comparative metabolomics to identify the endogenous ligands of DAF-12, a central regulator of development and adult

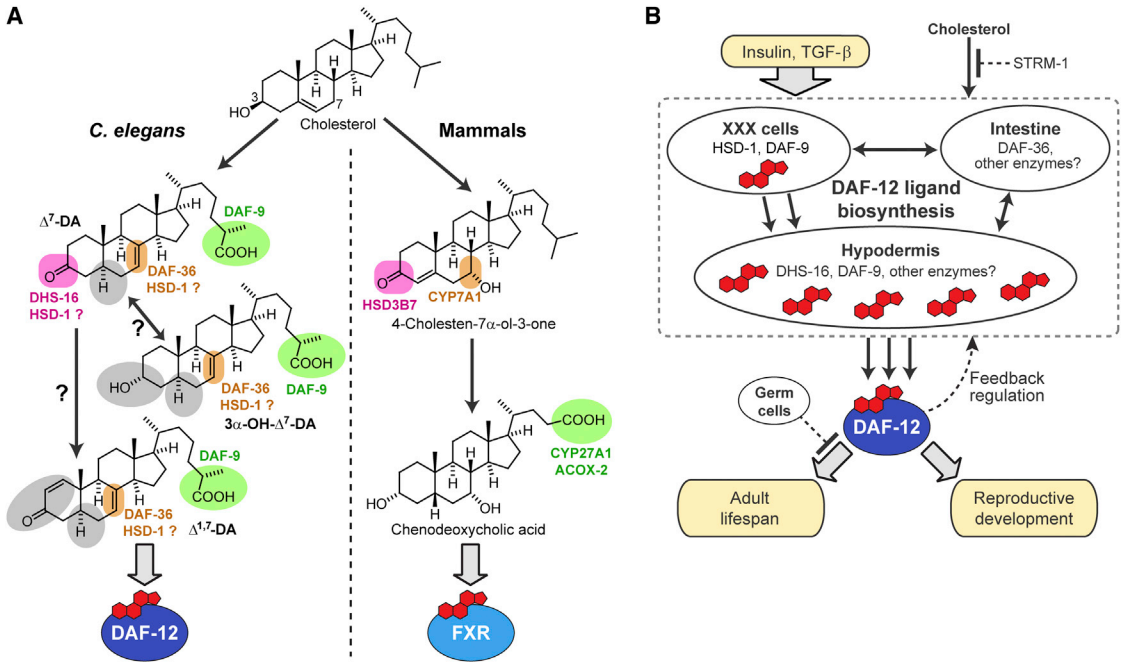

Figure 6. Comparison of NHR Signaling in Nematodes and Mammals and a Model for DAF-12 Signaling in *C. elegans*

(A) Comparison of NHR signaling in nematodes and mammals. In nematodes, oxidation or epimerization in position 3, oxidation in position 7, and side-chain oxidation produces ligands of DAF-12, whereas similar modification of the steroid skeleton in mammals produces bile acids that serve as ligands of farnesoid X receptor (FXR) (Russell, 2003) and possibly LXR (Theofilopoulos et al., 2013). Colors are used to highlight the functions of known enzymes in this pathway, whereas enzymes introducing the structural features highlighted in gray have not been described.

(B) Biosynthesis model for DAF-12 ligands regulating development and lifespan. Enzymes in the XXX cells downstream of insulin and TGF-β signaling produce small quantities of DAF-12 ligands, which trigger additional biosynthesis of DAF-12 ligands via upregulation of DAF-9 expression in the hypodermis, dependent on intestinally expressed DAF-36 and possibly other tissues. Although DAF-9 has been assumed to act directly upstream of DAF-12, our results suggest that DAF-9 may act on a variety of different substrates, including both 3-keto and 3-hydroxy sterols. Ligand biosynthesis is additionally regulated by STRM-1 and feedback through DAF-12. The lifespan-increasing effects of DAF-12 ligands depend on germ cell removal.

lifespan in *C. elegans* and an important model for ligand-regulated NHRs in higher animals. In contrast to earlier work that proposed (primarily based on screening candidate structures) Δ^4-DA and Δ^7-DA as endogenous DAF-12 ligands, our approach revealed $\Delta^{1,7}$-DA as the most abundant ligand in WT worms, in addition to smaller amounts of Δ^7-DA and 3α-OH-Δ^7-DA.

Steroids featuring a Δ^1-double bond have been described from very few natural sources (Wang et al., 2009a), although it is well known that introduction of Δ^1-unsaturation in natural 3-keto sterols (e.g., testosterone) can have pronounced effects on their activities (Counsell and Klimstra, 1962). Analyses of X-ray structures of the DAF-12 ligand binding domain complexed with DAs have demonstrated that small structural changes in the A and B rings of the bound steroid have significant effects on the ligand's affinity to DAF-12 (Wang et al., 2009b; Zhi et al., 2012), suggesting that specific modifications in the steroid A ring may serve to fine-tune DAF-12 transcriptional regulation. Identification of the enzyme(s) introducing the Δ^1-double bond will play an important role in elucidating functional differences between $\Delta^{1,7}$-DA and Δ^7-DA and may motivate reanalysis of mammalian metabolomes for the presence of endogenous Δ^1-steroids. The additional identification of the 3α-OH-Δ^7-DA creates a striking parallel to mammalian bile acid metabolism, which predominantly produces sterols with 3α configuration (Figure 6A) (Russell, 2003). Given its stereoselective biosynthesis by an as-of-yet unknown enzyme, it is likely that 3α-OH-Δ^7-DA serves specific functions in DAF-12 signaling. Notably, 3β-OH-Δ^7-DA, which was absent in WT worms but accumulated in *hsd-1; daf-22* and *daf-12* mutant worms, is much less active in both the in vivo and in vitro assays. However, it should be noted that both the transcriptional activation assay in mammalian cell culture (Figure 5B) and the AlphaScreen assay (Figure 5D) have limited cogency for judging the relative potency of different DAF-12 ligands in vivo, as both assays depend on recruitment of mammalian coactivators, such as SRC-1, whereas in vivo function of DAF-12 is thought to involve ligand-dependent dissociation of the endogenous *C. elegans* corepressor DIN-1 followed by binding of as-of-yet unidentified coactivators (Ludewig et al., 2004). The identification of multiple endogenous small-molecule regulators of DAF-12 in this study will accelerate the pursuit of currently elusive DAF-12 interactors and other components of DAF-12-dependent dauer and lifespan regulation.

Whereas it is well established that DAF-12 ligands are ultimately derived from dietary cholesterol, identification of $\Delta^{1,7}$-DA and 3α-OH-Δ^7-DA and the absence of Δ^4-DA necessitates revision of DAF-12 ligand biosynthesis models (Figures 1B and 6A). Our results indicate that DAF-36 as well as HSD-1 participate in the biosynthesis of Δ^7-DA and possibly $\Delta^{1,7}$-DA, whereas previously, HSD-1 had been assumed to function in Δ^4-DA biosynthesis. The finding that mutation of *dhs-16* affects

Δ^7-DA much more strongly than $\Delta^{1,7}$-DA production suggests that introduction of the 3-keto moiety in $\Delta^{1,7}$-DA may involve a different enzyme. Therefore, it appears that different DAF-12 ligands are produced via partially separate biosynthetic pathways, which is also supported by the finding that in *strm-1* mutants, Δ^7-DA production is increased to an extent much greater than that of $\Delta^{1,7}$-DA. Taken together, our identification of $\Delta^{1,7}$-DA, 3α-OH-Δ^7-DA, and Δ^0-DA indicates that several DAF-12 ligand biosynthetic enzymes remain to be identified.

C. elegans offers a unique opportunity to study the role of tissue-specific NHR ligand biosynthesis for endocrine signaling in a simple model system. Expression of DAF-12 ligand biosynthetic enzymes is thought to be controlled by insulin/IGF and TGF-β signaling; thus, ligand biosynthesis connects DAF-12 transcriptional regulation with these two highly conserved pathways (Figure 1A) (Wollam et al., 2012). The biosynthesis of multiple DAF-12 ligands via partially separate pathways suggests that different ligands may serve different functions (Arda et al., 2010). Notably, a recent study showed that DAF-12 ligands or ligand derivatives produced in the neuroendocrine XXX cells function as signaling molecules that trigger abundant additional ligand biosynthesis in the hypodermis, locking in organism-wide commitment to reproductive development (Figure 6B) (Gerisch and Antebi, 2004; Schaedel et al., 2012). Since the XXX cells are the primary sites of HSD-1 expression (Dumas et al., 2010; Patel et al., 2008), our finding that HSD-1 may contribute to Δ^7-DA biosynthesis supports a model in which XXX-produced Δ^7-DA (or derived 3α-OH-Δ^7-DA) triggers biosynthesis of large quantities of additional Δ^7-DA and $\Delta^{1,7}$-DA via *daf-36*, *dhs-16*, and hypodermal *daf-9* (Figure 6B). Ultimately, the elucidation of DAF-12 ligand biosynthetic pathways will require combining comparative metabolomics with tissue-specific manipulation of candidate genes. This will entail consideration of life-stage-specific aspects of ligand functions and biosynthesis, especially with regard to the intriguing role of DAF-12 ligands for adult longevity, which depends on additional signaling from the germline (Figure 6B) (Yamawaki et al., 2010).

DAF-12 ligands regulate adult longevity by activating microRNA targets that ultimately increase conserved DAF-16/FOXO transcriptional activity, thereby extending lifespan (Shen et al., 2012). Although the enzymes in DA biosynthesis are not strict orthologs of functionally corresponding enzymes in mammalian bile-acid biosynthesis, the striking similarities of steroidal NHR ligand biosynthetic pathways in nematodes and humans demonstrate the utility of *C. elegans* as a model organism for endocrine signaling (Figure 6A). Further functional characterization of the identified DAF-12 ligands will advance understanding of the roles of ligand-dependent NHRs in organism-wide coordination of metazoan development and aging. In addition, our study shows that NMR-based comparative metabolomics can provide detailed insight into metazoan small-molecule signaling pathways and that this approach can reveal signaling molecules and biosynthetic functions not suspected based on classical genetics and biochemical approaches. Finally, the DAF-12 ligands discovered here will yield important insights to combat parasitic infections, as parasitic nematodes use the DAF-12/DA signaling mechanism to regulate emergence from the infective stage (Ogawa et al., 2009; Wang et al., 2009b).

EXPERIMENTAL PROCEDURES

C. elegans Strains and Maintenance

Nematode stocks were maintained on nematode growth medium (NGM) plates made with Bacto Agar (BD Biosciences) and seeded with bacteria (*E. coli* OP50) at 20°C (http://www.wormbook.org/). *C. elegans* strains: WT (N2, Bristol), *daf-22(m130)*, *daf-22(ok693)*, *daf-9(dh6)*, *daf-9(dh6);daf-12(rh411rh61)*, *hsd-1(mg345)*, *hsd-1(mg433)*, *hsd-1(mg433);daf-22(ok693)*, *daf-36(k114)*, *daf-36(k114);daf-22(ok693)*, *dhs-16(tm1890)*, *dhs-16(tm1890);daf-22(m130)*, *strm-1(tm1781)*, *glp-1(e2141)*, *glp-1(e2141);daf-36(k114)*, *daf-12(rh411rh61)*. Compound mutants were constructed using standard techniques. Worms were grown at 20°C for at least two generations under replete conditions prior to liquid cultures.

Liquid Cultures

Worms from 4 10 cm NGM agar plates were washed using M9 medium into a 100 ml S complete medium preculture, where they were grown for 4 days at 22°C on a rotary shaker. Concentrated bacteria from 1 l of *E. coli* OP50 culture was added as food at days 1 and 3. On day 4, the preculture was divided equally into 16 500 ml Erlenmeyer flasks, each containing 100 ml of S complete medium. The resulting 16 cultures were grown for another 5 days at 22°C on a rotary shaker and continuously fed with concentrated bacteria, avoiding depletion of bacterial food at all times. The cultures were harvested on day 5 and centrifuged to separate supernatant media and worm pellets. At harvest, liquid cultures contained approximately 50%–70% L1–L3 worms. In liquid cultures grown for ~5 days at 22°C (at time of harvest), we observed 15%–20% dauers for N2, 2%–5% for *daf-22*, and none for *daf-9;daf-12* and *daf-12* mutants. *daf-36*, *dhs-16*, and *hsd-1* mutant worm cultures show 70%–95% dauers, whereas we observed less than 10% dauers in *daf-36;daf-22*, *dhs-16;daf-22*, and *hsd-1;daf-22* double-mutant cultures. The worm pellets were stored at −20°C until needed. Each 100 ml liquid culture yielded 2–3 ml of worm pellet, all of which was used for one replicate of metabolite extraction and analysis. At least three independent sets of cultures for *daf-22* and N2, and two for each of the steroid metabolism mutants, were used.

For DA analysis of synchronized cultures, gravid adults from 540 10 cm plates were washed with M9 buffer and treated with alkaline hypochlorite solution to isolate eggs. Eggs were washed twice with M9 buffer and hatched in fresh M9 for 24 hr. The synchronized L1 larvae were divided into two sets and transferred to S complete medium containing OP50. One set was allowed to grow for 25 hr at 20°C and 220 rpm, at which point the cultures were predominantly a 1:1 mixture of L2 and L3 larvae. A second set was grown for 48 hr and harvested when the culture contained a 9:1 mixture of L4 and young adults (YA). At the end of the specified growth period, the cultures were centrifuged at 4°C and the worm pellets stored at −20°C until processing for further analysis.

Preparation of Metabolome Extracts

The frozen worm pellets were added to precooled (−78°C) methanol (200 ml for each liquid culture and 20 ml for each staged culture) in a Waring blender and blended until no chunks remained. Methanol was evaporated in vacuo at 0°C –20°C, and the residue was resuspended in water (300 ml for liquid cultures and 25 ml for staged cultures). The resulting suspension was then lyophilized, and the residue was crushed to a fine powder using a mortar and pestle over 8 g of granular sodium chloride. The powder was then extracted twice with a 9:1 ethyl acetate:ethanol mixture (250 ml for samples obtained from liquid cultures and 25 ml for samples from staged liquid cultures) over 12 hr. The resulting suspension was filtered, and the filtrate was evaporated in vacuo at room temperature to produce the worm pellet metabolome extract used for chromatographic separations and analysis. For details, please see Supplemental Experimental Procedures.

NMR Spectroscopic Instrumentation and Analysis

NMR spectra were recorded on a Varian 900 MHz NMR Spectrometer equipped with a 5 mm ^{1}H (^{13}C/^{15}N) cryogenic probe, a Varian Inova 600 MHz NMR Spectrometer equipped with an HCN indirect detection probe, and a Varian Inova 500 MHz NMR Spectrometer equipped with a DBG broadband probe. Each spectrum was manually phased, baseline corrected, and calibrated to solvent peaks ($CHCl_3$ singlet at 7.26 ppm; CHD_2OD pseudoquintet at 3.31 ppm). Nongradient phase-cycled double-quantum filtered correlation

spectroscopy (DQF-COSY) spectra were acquired using the following parameters: 0.8 s acquisition time, 500–900 complex increments, 16–64 scans per increment. DQF-COSY spectra were zero filled to 8,192–16,384 × 4,096, and a cosine bell-shaped window function was applied in both dimensions before Fourier transformation. NMR spectra were processed using Varian VNMR, MestreLab's MestReC, and Mnova software packages. Dynamic range of the resulting spectra ranged from 300:1 to 500:1. For example, coupling constants could be determined for characteristic steroidal cross-peaks from DQF-COSY spectra containing as little as 5 μg $\Delta^{1,7}$-DA in a 2.5 mg metabolome fraction.

daf-9(dh6) Dauer Rescue Assay

Plate-based assay: metabolome fractions were resuspended in ethanol, mixed with 40 μl of 5× concentrated OP50 bacteria (from an overnight culture in lysogeny broth [LB] media), and plated on 3 cm plates containing 3 ml of NGM agar without added cholesterol. For rescue, ~100 eggs from a 4–8 hr egg lay were transferred onto the bacterial lawn and scored for dauer arrest at 27°C after 60 hr. For rescue experiments with synthetic steroids (0.1–500 nM tested), 10 μl compounds in ethanol (or ethanol alone) were mixed with 40 μl 5× concentrated OP50 bacteria and plated. Final concentrations include the total volume of agar (3 ml). We used 100 nM Δ^7-DA as a positive control. Additional rescue assays in liquid cultures were also carried out (for details, please refer to Supplemental Experimental Procedures). Data obtained from both plate-based and liquid culture assays are comparable. Figures in this paper are based on results from the plate-based assay.

Luciferase Assay for DAF-12 Transcriptional Activation

Luciferase assays to determine transcriptional activation of DAF-12 were performed as described earlier (Bethke et al., 2009). Briefly, HEK293T cells were seeded and transfected in 96-well plates with (per well) 30 ng transcription factor vector, 30 ng of GFP expression vector, 30 ng of luciferase reporter, and 5 ng β-galactosidase expression vector using the calcium phosphate precipitate method. Ethanol or ethanol solutions of ligands (synthetic DAs, 1–3,125 nM tested and metabolome fractions) were added 8 hr after transfection, and the luciferase and β-galactosidase activities were measured by a Synergy 2 BioTek LC Luminometer 16 hr after compound addition. We used 100 nM Δ^7-DA as a positive control. Data were processed using GEN5 software. Individual fractions were dried in vacuo and resuspended in 500 μl EtOH. We added 1 μl per 100 μl of media solution to each well.

AlphaScreen Assay for Direct Binding of DAF-12 Ligand Candidates

Direct binding of ligand candidates to DAF-12 was assessed using the AlphaScreen assay kit (PerkinElmer) as described previously (Motola et al., 2006). Also see Supplemental Experimental Procedures.

Statistical Analyses

All data, except for Figure 5D, are presented as mean ± SD. Data in Figure 5D are presented as mean ± SEM.

Nomenclature of DAF-12 Ligands

The IUPAC names for dafachronic acids as well as semirational constructs, such as 3α-hydroxy-Δ^7-dafachronic acid, are cumbersome, unlikely to be used consistently, and thus pose problems for text search algorithms and database curation. Therefore, we have obtained, for each of the identified dafachronic acid derivatives, unique *s*mall-*m*olecule *id*entifiers (SMIDs), from the *C. elegans* Small Molecule Identifier Database (SMID DB, http://smid-db.org/), an affiliate of Wormbase. SMIDs can be obtained for all newly identified *C. elegans* metabolites upon request. Thus, $\Delta^{1,7}$-DA, Δ^7-DA, 3α-OH-Δ^7-DA, Δ^4-DA, Δ^0-DA, and 3β-OH-Δ^7-DA have been named dafa#1, dafa#2, dafa#3, dafa#4, dafa#5, and dafa#6, respectively, as shown in Figure 4. To ensure effective curation, SMID DB recommends that the dafachronic acids be referred to by their respective SMIDs in subsequent publications.

SUPPLEMENTAL INFORMATION

Supplemental Information includes Supplemental Experimental Procedures, three figures, and three tables and can be found with this article online at http://dx.doi.org/10.1016/j.cmet.2013.11.024.

ACKNOWLEDGMENTS

We thank the Caenorhabditis Genetics Center (P40 OD010440) and Shohei Mitani (Tokyo Women's Medical University) for nematode strains. We thank D.N. Drechsel (MPI-CBG) for the purification of DAF-12. We thank A.S. Edison, J. Srinivasan, C. Coburn, and P. Sternberg for valuable suggestions. This work was supported in part by the National Institutes of Health (GM088290 and GM085285 to F.C.S., AG027498 to A.A., and T32GM008500 to J.C.J.), Cornell/Rockefeller/Sloan-Kettering Tri-Institutional Training Program in Chemical Biology (to N.B.), and the DFG (to A.B.). A.A. was additionally supported by the Ellison Medical Foundation, the MPG, and CECAD. K.J.D. received support from the Cellular and Molecular Biology Program at the UM Medical School and the UM Training Grant in the Biology of Aging. P.J.H. received support from the American Cancer Society (10-132-01). This study made use of NMRFAM, which is supported by NIH grants P41RR02301 (BRTP/ NCRR) and P41GM66326 (NIGMS).

Received: June 14, 2013
Revised: October 25, 2013
Accepted: November 22, 2013
Published: January 7, 2014

REFERENCES

Antebi, A. (2006). Nuclear hormone receptors in C. elegans. WormBook, 1–13.

Antebi, A., Yeh, W.H., Tait, D., Hedgecock, E.M., and Riddle, D.L. (2000). daf-12 encodes a nuclear receptor that regulates the dauer diapause and developmental age in C. elegans. Genes Dev. *14*, 1512–1527.

Arda, H.E., Taubert, S., MacNeil, L.T., Conine, C.C., Tsuda, B., Van Gilst, M., Sequerra, R., Doucette-Stamm, L., Yamamoto, K.R., and Walhout, A.J. (2010). Functional modularity of nuclear hormone receptors in a Caenorhabditis elegans metabolic gene regulatory network. Mol. Syst. Biol. *6*, 367.

Bethke, A., Fielenbach, N., Wang, Z., Mangelsdorf, D.J., and Antebi, A. (2009). Nuclear hormone receptor regulation of microRNAs controls developmental progression. Science *324*, 95–98.

Brown, A.J., and Slatopolsky, E. (2008). Vitamin D analogs: therapeutic applications and mechanisms for selectivity. Mol. Aspects Med. *29*, 433–452.

Butcher, R.A., Ragains, J.R., Li, W., Ruvkun, G., Clardy, J., and Mak, H.Y. (2009). Biosynthesis of the Caenorhabditis elegans dauer pheromone. Proc. Natl. Acad. Sci. USA *106*, 1875–1879.

Counsell, R.E., and Klimstra, P.D. (1962). Anabolic agents: derivatives of 2-Halo 5alpha-Androst-1-Ene. J. Med. Pharm. Chem. *91*, 477–483.

Dumas, K.J., Guo, C., Wang, X., Burkhart, K.B., Adams, E.J., Alam, H., and Hu, P.J. (2010). Functional divergence of dafachronic acid pathways in the control of C. elegans development and lifespan. Dev. Biol. *340*, 605–612.

Fielenbach, N., and Antebi, A. (2008). C. elegans dauer formation and the molecular basis of plasticity. Genes Dev. *22*, 2149–2165.

Forseth, R.R., and Schroeder, F.C. (2011). NMR-spectroscopic analysis of mixtures: from structure to function. Curr. Opin. Chem. Biol. *15*, 38–47.

Gems, D., Sutton, A.J., Sundermeyer, M.L., Albert, P.S., King, K.V., Edgley, M.L., Larsen, P.L., and Riddle, D.L. (1998). Two pleiotropic classes of daf-2 mutation affect larval arrest, adult behavior, reproduction and longevity in Caenorhabditis elegans. Genetics *150*, 129–155.

Gerisch, B., and Antebi, A. (2004). Hormonal signals produced by DAF-9/cytochrome P450 regulate C. elegans dauer diapause in response to environmental cues. Development *131*, 1765–1776.

Gerisch, B., Weitzel, C., Kober-Eisermann, C., Rottiers, V., and Antebi, A. (2001). A hormonal signaling pathway influencing C. elegans metabolism, reproductive development, and life span. Dev. Cell *1*, 841–851.

Gerisch, B., Rottiers, V., Li, D., Motola, D.L., Cummins, C.L., Lehrach, H., Mangelsdorf, D.J., and Antebi, A. (2007). A bile acid-like steroid modulates Caenorhabditis elegans lifespan through nuclear receptor signaling. Proc. Natl. Acad. Sci. USA *104*, 5014–5019.

Hammell, C.M., Karp, X., and Ambros, V. (2009). A feedback circuit involving let-7-family miRNAs and DAF-12 integrates environmental signals and developmental timing in Caenorhabditis elegans. Proc. Natl. Acad. Sci. USA *106*, 18668–18673.

Hannich, J.T., Entchev, E.V., Mende, F., Boytchev, H., Martin, R., Zagoriy, V., Theumer, G., Riezman, I., Riezman, H., Knölker, H.J., and Kurzchalia, T.V. (2009). Methylation of the sterol nucleus by STRM-1 regulates dauer larva formation in Caenorhabditis elegans. Dev. Cell *16*, 833–843.

Heery, D.M., Kalkhoven, E., Hoare, S., and Parker, M.G. (1997). A signature motif in transcriptional co-activators mediates binding to nuclear receptors. Nature *387*, 733–736.

Held, J.M., White, M.P., Fisher, A.L., Gibson, B.W., Lithgow, G.J., and Gill, M.S. (2006). DAF-12-dependent rescue of dauer formation in Caenorhabditis elegans by (25S)-cholestenoic acid. Aging Cell *5*, 283–291.

Hsin, H., and Kenyon, C. (1999). Signals from the reproductive system regulate the lifespan of C. elegans. Nature *399*, 362–366.

Hu, P.J. (2007). Dauer. WormBook, 1–19.

Jia, K., Albert, P.S., and Riddle, D.L. (2002). DAF-9, a cytochrome P450 regulating C. elegans larval development and adult longevity. Development *129*, 221–231.

Kenyon, C. (2010). A pathway that links reproductive status to lifespan in Caenorhabditis elegans. Ann. N Y Acad. Sci. *1204*, 156–162.

Larsen, P.L., Albert, P.S., and Riddle, D.L. (1995). Genes that regulate both development and longevity in Caenorhabditis elegans. Genetics *139*, 1567–1583.

Ludewig, A.H., Kober-Eisermann, C., Weitzel, C., Bethke, A., Neubert, K., Gerisch, B., Hutter, H., and Antebi, A. (2004). A novel nuclear receptor/coregulator complex controls C. elegans lipid metabolism, larval development, and aging. Genes Dev. *18*, 2120–2133.

Mangelsdorf, D.J., Thummel, C., Beato, M., Herrlich, P., Schütz, G., Umesono, K., Blumberg, B., Kastner, P., Mark, M., Chambon, P., and Evans, R.M. (1995). The nuclear receptor superfamily: the second decade. Cell *83*, 835–839.

Motola, D.L., Cummins, C.L., Rottiers, V., Sharma, K.K., Li, T., Li, Y., Suino-Powell, K., Xu, H.E., Auchus, R.J., Antebi, A., and Mangelsdorf, D.J. (2006). Identification of ligands for DAF-12 that govern dauer formation and reproduction in C. elegans. Cell *124*, 1209–1223.

Ogawa, A., Streit, A., Antebi, A., and Sommer, R.J. (2009). A conserved endocrine mechanism controls the formation of dauer and infective larvae in nematodes. Curr. Biol. *19*, 67–71.

Palanker, L., Tennessen, J.M., Lam, G., and Thummel, C.S. (2009). Drosophila HNF4 regulates lipid mobilization and β-oxidation. Cell Metab. *9*, 228–239.

Patel, D.S., Fang, L.L., Svy, D.K., Ruvkun, G., and Li, W. (2008). Genetic identification of HSD-1, a conserved steroidogenic enzyme that directs larval development in Caenorhabditis elegans. Development *135*, 2239–2249.

Pungaliya, C., Srinivasan, J., Fox, B.W., Malik, R.U., Ludewig, A.H., Sternberg, P.W., and Schroeder, F.C. (2009). A shortcut to identifying small molecule signals that regulate behavior and development in Caenorhabditis elegans. Proc. Natl. Acad. Sci. USA *106*, 7708–7713.

Riddle, D.L., and Albert, P.S. (1997). Genetic and environmental regulation of dauer larva development. In C elegans II, D.L. Riddle, T. Blumenthal, B.J. Meyer, and J.R. Priess, eds. (Cold Spring Harbor: Cold Spring Harbor Laboratory Press).

Riddle, D.L., Swanson, M.M., and Albert, P.S. (1981). Interacting genes in nematode dauer larva formation. Nature *290*, 668–671.

Rottiers, V., Motola, D.L., Gerisch, B., Cummins, C.L., Nishiwaki, K., Mangelsdorf, D.J., and Antebi, A. (2006). Hormonal control of C. elegans dauer formation and life span by a Rieske-like oxygenase. Dev. Cell *10*, 473–482.

Russell, D.W. (2003). The enzymes, regulation, and genetics of bile acid synthesis. Annu. Rev. Biochem. *72*, 137–174.

Schaedel, O.N., Gerisch, B., Antebi, A., and Sternberg, P.W. (2012). Hormonal signal amplification mediates environmental conditions during development and controls an irreversible commitment to adulthood. PLoS Biol. *10*, e1001306.

Schupp, M., and Lazar, M.A. (2010). Endogenous ligands for nuclear receptors: digging deeper. J. Biol. Chem. *285*, 40409–40415.

Shen, Y., Wollam, J., Magner, D., Karalay, O., and Antebi, A. (2012). A steroid receptor-microRNA switch regulates life span in response to signals from the gonad. Science *338*, 1472–1476.

Singarapu, K.K., Zhu, J., Tonelli, M., Rao, H., Assadi-Porter, F.M., Westler, W.M., DeLuca, H.F., and Markley, J.L. (2011). Ligand-specific structural changes in the vitamin D receptor in solution. Biochemistry *50*, 11025–11033.

Taubert, S., Ward, J.D., and Yamamoto, K.R. (2011). Nuclear hormone receptors in nematodes: evolution and function. Mol. Cell. Endocrinol. *334*, 49–55.

Theofilopoulos, S., Wang, Y., Kitambi, S.S., Sacchetti, P., Sousa, K.M., Bodin, K., Kirk, J., Saltó, C., Gustafsson, M., Toledo, E.M., et al. (2013). Brain endogenous liver X receptor ligands selectively promote midbrain neurogenesis. Nat. Chem. Biol. *9*, 126–133.

von Reuss, S.H., Bose, N., Srinivasan, J., Yim, J.J., Judkins, J.C., Sternberg, P.W., and Schroeder, F.C. (2012). Comparative metabolomics reveals biogenesis of ascarosides, a modular library of small-molecule signals in C. elegans. J. Am. Chem. Soc. *134*, 1817–1824.

Wang, W., Lee, J.S., Nakazawa, T., Ukai, K., Mangindaan, R.E., Wewengkang, D.S., Rotinsulu, H., Kobayashi, H., Tsukamoto, S., and Namikoshi, M. (2009a). (25S)-cholesten-26-oic acid derivatives from an Indonesian soft coral Minabea sp. Steroids *74*, 758–760.

Wang, Z., Zhou, X.E., Motola, D.L., Gao, X., Suino-Powell, K., Conneely, A., Ogata, C., Sharma, K.K., Auchus, R.J., Lok, J.B., et al. (2009b). Identification of the nuclear receptor DAF-12 as a therapeutic target in parasitic nematodes. Proc. Natl. Acad. Sci. USA *106*, 9138–9143.

Williams, T.W., Dumas, K.J., and Hu, P.J. (2010). EAK proteins: novel conserved regulators of C. elegans lifespan. Aging (Albany, N.Y. Online) *2*, 742–747.

Wollam, J., and Antebi, A. (2011). Sterol regulation of metabolism, homeostasis, and development. Annu. Rev. Biochem. *80*, 885–916.

Wollam, J., Magomedova, L., Magner, D.B., Shen, Y., Rottiers, V., Motola, D.L., Mangelsdorf, D.J., Cummins, C.L., and Antebi, A. (2011). The Rieske oxygenase DAF-36 functions as a cholesterol 7-desaturase in steroidogenic pathways governing longevity. Aging Cell *10*, 879–884.

Wollam, J., Magner, D.B., Magomedova, L., Rass, E., Shen, Y., Rottiers, V., Habermann, B., Cummins, C.L., and Antebi, A. (2012). A novel 3-hydroxysteroid dehydrogenase that regulates reproductive development and longevity. PLoS Biol. *10*, e1001305.

Yamawaki, T.M., Berman, J.R., Suchanek-Kavipurapu, M., McCormick, M., Gaglia, M.M., Lee, S.J., and Kenyon, C. (2010). The somatic reproductive tissues of C. elegans promote longevity through steroid hormone signaling. PLoS Biol. *8*, 8.

Yoshiyama-Yanagawa, T., Enya, S., Shimada-Niwa, Y., Yaguchi, S., Haramoto, Y., Matsuya, T., Shiomi, K., Sasakura, Y., Takahashi, S., Asashima, M., et al. (2011). The conserved Rieske oxygenase DAF-36/Neverland is a novel cholesterol-metabolizing enzyme. J. Biol. Chem. *286*, 25756–25762.

Zhi, X., Zhou, X.E., Melcher, K., Motola, D.L., Gelmedin, V., Hawdon, J., Kliewer, S.A., Mangelsdorf, D.J., and Xu, H.E. (2012). Structural conservation of ligand binding reveals a bile acid-like signaling pathway in nematodes. J. Biol. Chem. *287*, 4894–4903.